Journal of Alloys and Compounds 617 (2014) 277–280

Contents lists available at ScienceDirect

Journal of Alloys and Compounds

journal homepage: www.elsevier.com/locate/jalcom

Tension–compression yield asymmetry in as-cast magnesium alloy

Sung Hyuk Park [a,*], Jeong Hun Lee [b], Byoung Gi Moon [a], Bong Sun You [a]

[a] Light Metal Division, Korea Institute of Materials Science (KIMS), Changwon 642-831, Republic of Korea
[b] Department of Materials Science and Engineering, Pohang University of Science and Technology (POSTECH), Pohang 790-784, Republic of Korea

ARTICLE INFO

Article history:
Received 3 June 2014
Received in revised form 16 July 2014
Accepted 21 July 2014
Available online 7 August 2014

Keywords:
Magnesium alloys
Texture
Yield asymmetry
Twinning
Schmid factor

ABSTRACT

The tension–compression asymmetry in a randomly textured cast magnesium alloy is investigated in terms of its {10–12} twinning characteristics. This {10–12} twinning behavior, which governs the initial stages of deformation, is found to be notably different under tension and compression, consequently resulting in a lower yield strength and higher strain hardening under tension than compression. An interpretation of this behavior is provided through subsequent analysis of the Schmid factor, the grain fraction favorable for twinning, and the dominant twinning mechanism.

1. Introduction

Unlike cubic metals with symmetrical crystal structures, most magnesium (Mg) alloys exhibit different yield strengths under tension and compression [1]. In particular, wrought Mg alloys tend to display a significant tension–compression yield asymmetry, which is attributed to the combined effect of their texture and the polar nature of deformation twinning [2]. Most wrought Mg alloys have a strong basal texture, in which the majority of basal planes are aligned parallel to the direction of the fabrication process used (e.g., extrusion, rolling, etc.). Since {10–12} extension twinning is activated under tension parallel to the *c*-axis of the hexagonal close-packed unit cell, or compression perpendicular to the *c*-axis [3], it only occurs in compression along the process direction and thus leads to a significant low compressive yield strength. While, slip-dominant deformation in tension results in a relatively high yield strength. This asymmetric yield phenomenon is well established in wrought Mg alloys, and extensive research has been conducted to reduce it by controlling microstructural characteristics (e.g., grain refinement, texture randomization, precipitate formation, etc.) through various methods such as the addition of rare earth elements [4], severe plastic deformation [5], and annealing [6].

Tension–compression yield asymmetry has also been recently reported in cast Mg alloys [7–10], although they show less asymmetry than wrought Mg alloys. However, given that cast Mg alloys are generally considered to have random texture, the yield asymmetry mechanism for wrought Mg alloys cannot be applied to them [7]. Instead, it is known that the asymmetry in cast Mg alloys is related to its {10–12} twinning behavior in tension and compression [8]. For instance, Máthis et al. [9] have reported that for a cast Mg alloy, twin nucleation is observed during the whole tensile test period, while it is observed only at the beginning of deformation and the subsequent strain causes twin growth. This difference in twinning behavior under tension and compression has been directly observed by several techniques, such as the neutron diffraction [9] and acoustic emission [9,10], together with conventional microstructural observation [7]. However, the detailed characteristics of {10–12} twinning activation under tension and compression, and the resultant deformation behavior, have not yet been systematically investigated.

In this study, therefore, we explored why the {10–12} twinning and yielding behavior is different under tension and compression in a randomly textured cast Mg alloy. For this purpose, the twinning characteristics under tensile and compressive deformation were compared in terms of the Schmid factor (SF) and grain fraction favorable for twinning, and the activated twin variants; their relationship to the yielding and hardening behavior was also discussed.

2. Experimental procedure

A billet of commercial AZ31 (Mg–3 wt% Al–1 wt% Zn) alloy was prepared using a previously described method [11]. This cast billet was homogenized at 400 °C for 15 h, then water-quenched. The homogenized material had a twin-free equiaxed grain structure with an average linear-intercept grain size of ∼450 μm (Fig. 1a).

* Corresponding author. Tel.: +82 55 280 3516; fax: +82 55 280 3599.
E-mail address: shpark@kims.re.kr (S.H. Park).

http://dx.doi.org/10.1016/j.jallcom.2014.07.164
0925-8388/

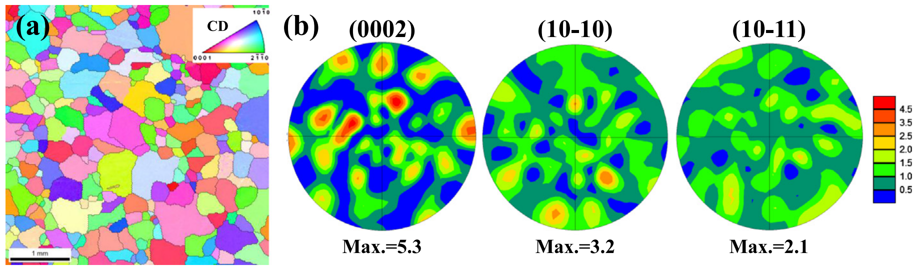

Fig. 1. Microstructural characteristics of a cast AZ31 Mg alloy: (a) inverse pole figure map and (b) (0002), (10–10), and (10–11) pole figures.

The initial texture of the material, as measured by electron backscatter diffraction (EBSD), showed no preferred orientation (Fig. 1b). The relatively high maximum-intensity values (2.1–5.3) of the pole figures appear to result from the limited measuring area of 19.7 mm^2. The results of X-ray diffraction confirm that the cast material has a nearly random texture; the average relative intensities of the (0002), (10–10), and (10–11) peaks ($I_{(0002)}$:$I_{(10-10)}$:$I_{(10-11)}$ = 1:0.78:2.81) were comparable to those of a completely random Mg powder ($I_{(0002)}$:$I_{(10-10)}$:$I_{(10-11)}$ = 1:0.85:2.44).

Since it is known that cylindrical specimens can cause an inhomogeneous deformation field during compression, thereby inducing experimental error in the stress–strain curve, both tensile and compressive tests were conducted using dog-bone-shaped specimens to prevent stress concentration from loading machine connections and to ensure a homogeneous distribution of stress and strain within the measurement region (i.e., gage section). These specimens had a gauge length and diameter of 10 and 5 mm, respectively, and they were machined from the homogenized billet along three directions: the casting direction (CD) and two orthogonal directions perpendicular to the CD (denoted as "0°" and 90°"), as shown in Fig. 2a. All tests were conducted at room temperature and a strain rate of 10^{-3} s^{-1}, using an INSTRON 8801 testing machine. An extensometer with an 8.75 mm gage-length was used in all tests to obtain the exact strain within the homogeneously deformed region. Specimens for EBSD examination were ground with 2400 grit silicon carbide paper and polished using 1 lm diamond paste, followed by a final polish with colloidal silica to remove surface strains and provide a high quality surface finish. They were then examined by an EBSD installed in a field emission scanning electron microscope (Hitachi, SU-6600) operating at an accelerating voltage of 20 kV with a working distance of 20 mm, and which was fitted with a TSL™ EBSD camera to identify the active twin variant of deformed samples. Automated EBSD scans of a 3.77 mm^2 area were performed in stage control mode with a step size of 3 μm using TSL data acquisition software. The resulting inverse pole figure (IPF) map, crystallographic orientation analysis, and (0001), (10–10), and (10–11) pole figures were processed with commercial TSL OIM software. The resulting EBSD data was one-step cleaned using grain dilation (clean-up parameters: grain tolerance angle = 5 and minimum grain size = 2), and was then analyzed using only those data points with a confidence index > 0.1.

3. Results and discussion

The stress–strain curves and strain hardening rate curves obtained under tension and compression along each of the three loading directions are presented in Fig. 2. It can be seen that the tensile and compressive flow curves for each of the samples are essentially identical in appearance, further confirming the random texture of the cast material. However, there is a notable difference in the tensile and compressive behavior during the early stages of deformation, especially in the vicinity of the yield point: Firstly, the cast AZ31 billet yields at a significantly lower stress in tension; the 0.2% offset yield strengths, as determined from the experimental Young's modulus fitted to the initial part of the stress–strain curves, are 37 in tension and 65 MPa in compression. Consequently, the ratio of compressive yield strength to tensile yield strength (i.e., asymmetry ratio) of 1.76 for the cast AZ31 alloy is much greater than the ~0.5 of wrought AZ31 alloys [12]. Secondly, the compressive flow curves show a relatively distinct yield point after rapid hardening in the elastic region, whereas the tensile curves reveal an ambiguous elastic–plastic transition due to the initial yielding at very low stress and subsequent continuous hardening (Fig. 2a). Finally, the strain hardening that occurs immediately after yielding is greater in tension than in compression; the strain hardening rate gradually decreases up to a strain of ~2% in tension, but decreases much more rapidly during early deformation to ~0.5% in compression (Fig. 2b).

This asymmetric yield behavior of the cast material originates from the difference in {10–12} twinning characteristics under tensile and compressive loading, because slip-induced deformation is independent of the loading direction [7,8]. To compare the twinning activities in tension and compression, the SF values of the {10–12} twinning system were calculated as a function of the angle, θ, between the loading axis and c-axis (Fig. 3a). It should be noted here that SF is also dependent on the angle, α, between the loading axis and a-axis [13]; a randomly-textured polycrystalline Mg alloy exhibits angle ranges of $0° \leqslant \theta \leqslant 90°$ and $0° \leqslant \alpha \leqslant 30°$. Thus, for the simplicity of calculation, two extreme cases of $\alpha = 0°$ and $\alpha = 30°$, which correspond to the maximum or minimum SF value, were considered (detailed definitions of θ

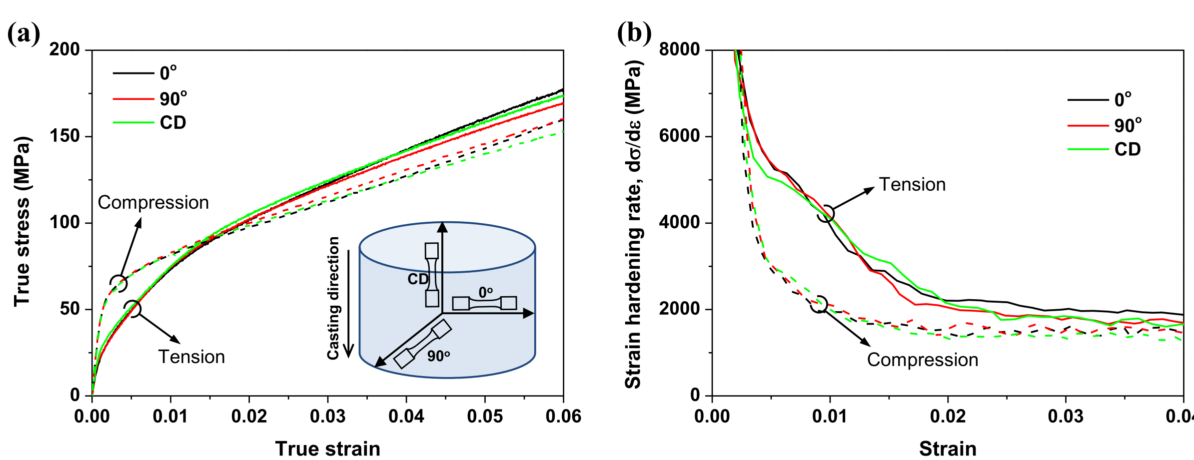

Fig. 2. Deformation characteristics of a cast AZ31 Mg alloy under tension and compression: (a) true stress–strain curve and (b) strain hardening rate curve. The inset of (a) shows tensile and compressive samples with three orthogonal loading axes machined from a homogenized billet.